A REPLICABLE OPEN-SOURCE MULTI-CAMERA SYSTEM FOR LOW-COST 4D GLACIER MONITORING

F. Ioli [1]*, E. Bruno [2], D. Calzolari [3], M. Galbiati [4], A. Mannocchi [5], P. Manzoni [6], M. Martini [7] A. Bianchi [1], A. Cina [8], C. De Michele [1], L. Pinto [1]

[1] Politecnico di Milano, Department of Civil and Environmental Engineering, Milan, Italy
[2] Politecnico di Torino, Department of Mechanical and Aerospace Engineering, Torino, Italy
[3] CERN, Geneva, Switzerland
[4] Politecnico di Milano, Department of Energy, Milan, Italy
[5] Politecnico di Milano, Department of Aerospace Science and Technology, Milan, Italy
[6] Politecnico di Milano, Department of Mathematics, Milan, Italy
[7] Politecnico di Torino, Department of Electronics and Telecommunications, Torino, Italy
[8] Politecnico di Torino, Department of Environment, Land and Infrastructure Engineering, Torino, Italy

KEY WORDS: Stereo photogrammetry, Time-lapse, Glaciers, Structure-from-Motion, Embedded systems, Rasperry Pi, Arduino

ABSTRACT:

Image-based monitoring has emerged as a prevalent technique for sensing mountain environments. Monoscopic time-lapse cameras, which rely on digital image correlation to quantify glacier motion, have limitations due to the need for a Digital Elevation Model for deriving 3D flow velocity fields. Multi-camera systems overcome this limitation, as they allow for a 3D reconstruction of the scene. This paper presents a replicable low-cost stereoscopic system designed for 4D glacier monitoring. The system consists of independent and autonomous units, built from off-the-shelves components, such as a DSLR camera, an Arduino microcontroller, and a Raspberry Pi Zero, reducing costs compared to pre-built time-lapse cameras. The units are energetically self-sufficient and resistant to harsh alpine conditions. The system was successfully tested for more than a year to monitor the northwest terminus of the Belvedere Glacier (Italian Alps). Daily stereo-pairs acquired were processed with Structure-from-Motion to derive 3D point clouds of the glacier terminus and estimate glacier retreat and ice volume loss. By combining the information about ice volume loss with ablation estimates and ice flow velocity information, e.g., derived from monoscopic-camera time series, a multi-camera system enables a comprehensive understanding of sub-seasonal glacier dynamics.

1. INTRODUCTION

Glacier monitoring in high alpine environments is an essential task for understanding climate change and its effects on natural systems (Barry, 2006, Zemp et al., 2006). Recently, photogrammetry and Structure-from-Motion (SfM) have become increasingly popular tools for 3D reconstruction and monitoring of remote and inaccessible areas, such as high alpine glaciers (Piermattei et al., 2016). Although UAV-based photogrammetry is a cost-effective solution for acquiring high-resolution and accurate 3D models of mountain environments (Chudley et al., 2019, Ioli et al., 2021), it still requires in-situ human intervention, which can be troublesome for long-term monitoring activities. In contrast, fixed time-lapse cameras are designed to operate autonomously and provide images with high temporal frequency (e.g., daily) for long periods, requiring minimal maintenance. These cameras can serve as webcams for monitoring and collecting both qualitative and quantitative data on dynamic scenes, especially in remote alpine areas.

In combination with computer vision and image processing techniques, low-cost time-lapse cameras have been effectively employed for various applications, including monitoring glaciers and ice cliffs (Giordan et al., 2016, Schwalbe and Maas, 2017, Kneib et al., 2022), observing calving glaciers (Vallot et al., 2019), estimating snow accumulation and melting (Ide and Oguma, 2013), measuring streams' and rivers' discharge (Young et al., 2015), monitoring landslide (Roncella et al., 2014), and geomorphological sensing (Eltner et al., 2017). For what concerns glacier monitoring, several software packages which utilize Digital Image Correlation (DIC) and feature tracking to estimate glacier surface velocity from terrestrial time-lapse cameras have been developed. For instance, ImGraft (Messerli and Grinsted, 2015) and Pointcatcher (James et al., 2016) are well-known MATLAB packages for feature tracking and geo-referencing velocity vectors onto Digital Elevation Models (DEMs). More recently, PyTrx (How et al., 2020), a Python toolbox for calculating real-world measurements from oblique time-lapse images, and LAMMA (Dematteis et al., 2022), a local adaptive multiscale image matching algorithm, were released.

A large part of the existing literature exclusively considers single-camera systems for image acquisition. While this option may seem practical due to ease of installation and cost-effectiveness, it ultimately hinders the employment of standard photogrammetric techniques for computing 3D models and deriving 3D velocity fields of moving objects. Indeed, when a single camera is used to derive surface velocities, an external DEM must be provided in order to georeference the pixel-wise displacements obtained from the images by DIC. Roncella et al. (Roncella et al., 2014) first developed a low-cost and handmade stereoscopic system for continuous monitoring of a landslide. They proposed using a fully photogrammetric approach to derive a 3D model of the scene during every image acquisition, eliminating the need for a priori DEMs. More recently, stereoscopic (Marsy et al., 2020) or multi-camera (Kneib et al.,

* Corresponding author

2022) systems have been tested in a remote glacial environment. However, these studies focused more on the image processing methods and results than on the implementation of the system, providing minimal or no information on the hardware used.

An alpine glacier is a hazardous and challenging environment for the installation of monitoring systems. Considering logistical factors, human intervention should be kept to its bare minimum. Any monitoring system should be capable of withstanding extreme cold temperatures and acquiring data autonomously. In addition, it must be designed to be self-sufficient in terms of power usage: low energy consumption has to be a primary requirement in the design of a monitoring system, both in terms of hardware and data acquisition algorithm.

The aim of this work is to provide a general framework for the realization of low-cost-and-low-power multi-camera monitoring systems. The complete architecture of a low-cost stereoscopic system based on two time-lapse cameras for continuously monitoring an alpine glacier is presented. The setup was successfully tested for over a year on the northwest terminus of the debris-covered Belvedere Glacier in the Italian Alps. Overall, it proved to be accurate and robust in performance, allowing for the continuous data collection necessary for high-frequency monitoring of the remote glacier. Additionally, the system’s open-source design enables easy replication for further research studies conducted in other hazardous environments.

2. SYSTEM DESCRIPTION

The low-cost stereoscopic system for continuous monitoring is composed of two independent units, each housing an off-the-shelves DSLR camera. Each unit consists in an autonomous monitoring station that provides power supply, internet connectivity, timing and scheduling of image acquisition, and protection from the harsh environment. The station was designed and built adapting to the alpine environment an existing open-source model developed by Greig Sheridan and published in the GitHub repository `https://github.com/greiginsydney` (Sheridan, 2021). A key aspect of the project was to ensure easy assembly and realization of the system to guarantee future replication or improvement by non-experts. In the following, we describe in detail the services and the nominal performances provided by our system that make it worth consideration for applications in different monitoring contexts. Refer to Figure 1 for a descriptive schematic of the whole system showing the components selected for the Belvedere Glacier case study. The choice of the camera and optics is discussed in Section 3, as these components are dependent on the domain of use of the stereoscopic system.

2.1 Power supply

Each monitoring unit has its autonomous power supply line (yellow arrows in Figure 1) provided by a solar panel combined with a sealed lead-acid battery. An MPPT (Maximum Power Point Tracker) charge regulator directly connects with the unit’s internal circuit, providing a regular current supply to the battery and the load and exploiting all the power generated by the panel. This regulator prevents any excess current that may damage the connected device, thus increasing the reliability of the system. Its battery life-saving algorithm modulates the load disconnection level so that a nearly 100% recharge is achieved about once every week and, in case of battery discharging, the whole system is switched off until 100% recharge of

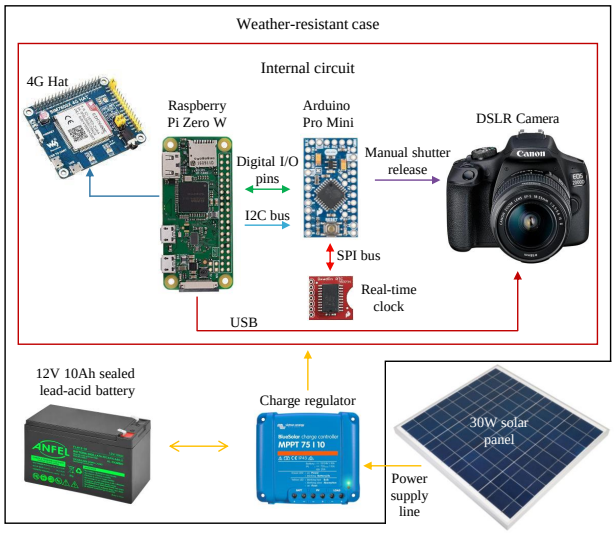

Figure 1. Scheme of the proposed acquisition system configuration for a single monitoring station. Arrows indicate the direction of signal initiation. Image adapted from Greig Sheridan (Sheridan, 2021).

the battery is achieved. The whole monitoring system is designed to minimise power consumption, e.g., by powering off devices responsible for the highest power consumption when not needed. An estimation of the system’s energy consumption guided the choice of the components of the power supply line. Specifically, the battery and the associated panel must be accurately dimensioned for the system’s purpose. To this end, the Photovoltaic Geographical Information System (PVGIS) (EU Science Hub, 2022), a tool provided by the European Commission, was used. PVGIS can estimate the performance of off-grid photovoltaic systems according to the installation site and it is supported by a database and algorithms for calculating solar radiation. Tuning the parameters for the Belvedere Glacier location and the system consumption, we ended up with the specifications of solar panel power of 30 W and battery voltage of 12 V and capacity of 10 Ah. Some compromises were made, accepting that the system would not be sufficiently powered in the months with lowest solar radiation (November, December, January, and February). In Section 3, further details on PVGIS simulations for the Belvedere Glacier case study are given.

2.2 System control and scheduling

The internal electronic circuit (red box in Figure 1) of the monitoring unit is the only load connected to the power supply and is responsible for all the system’s control and scheduling functionalities. Its components are a real-time clock (number 3 in Figure 2) with a 12 mm coin-cell backup battery, an Arduino microcontroller (Pro Mini 328 3.3V 8MHz, number 4 in Figure 2), a Raspberry Pi Zero W with 128 GB SD memory card (number 6 in Figure 2), and minor elements for connections, isolation (capacitors and optoisolators numbers 1 and 5 in Figure 2), and voltage regulations (numbers 2 in Figure 2). The circuit was realized manually by soldering wires and components on a stripboard (see Figure 2).

The Arduino communicates through an SPI (Serial Peripheral Interface) bus with an accurate real-time clock to schedule its actions: waking the camera, firing the shutter to take a photo, and turning on/off the Raspberry. The Raspberry is able to access the camera images and transfer them to a remote server

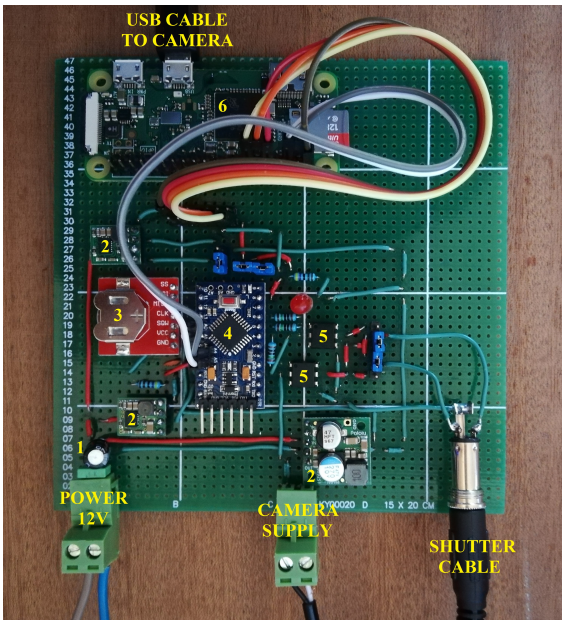

Figure 2. Stripboard on which are soldered the main components of the internal circuit: capacitors (1), voltage regulators (2), real-time clock with coin-cell battery (3), Arduino Pro Mini (4), optoisolators (5), and Raspberry Pi Zero W (6).

via internet connectivity. A large storage memory is added to the unit to save photos before remote transferring. The Raspberry also provides a web-based, user-friendly interface (Figure 3) to configure and monitor the system remotely (Sheridan, 2021). An I2C (Inter Integrated Circuit) bus and digital pin connections enable higher-level communication between these two boards. Among the minor components, we mention the role of the three voltage regulators. They allow each unit to be powered at the appropriate voltage and current: starting from the 12 V in input, one delivers 3.3 V and 500 mA to the Arduino, one 5 V and 2.5 A to the Raspberry and its hat, and the other 7.5 V and 2.4 A to the camera. The Arduino controls the 5V regulator of the Raspberry to reduce quiescent power consumption when the Raspberry board is off.

Acquisition of a defined number of images, camera triggering and timing, and sending of images to a remote server can be scheduled thanks to adequate programming of a cyclic executive program in C++ for Arduino and of services executing automatically Python scripts for the Raspberry. All the monitoring station activities can be remotely scheduled from the terminal or a user-friendly web interface (Sheridan, 2021). This useful feature allows one to change the settings and check the behaviour of the system, avoiding the need for manual intervention. The Raspberry uses the gPhoto2, a Python-based protocol developed to specifically interact with popular cameras’ firmware, to communicate with the camera and access the new photos. The web-based interface service is based on NGINX and Gunicorn, open-source software for web servers. The interface (Figure 3) consists of a web page accessible with credentials and provides a summary of the system state and the exact time of the last operations (time of the last shot and the last upload of images), temperatures of the components, previews of the last images, buttons to wake up the camera, take a preview photo and schedule the system routine (time and number of photo acquisition, wake-up time of the Raspberry) and some camera settings.

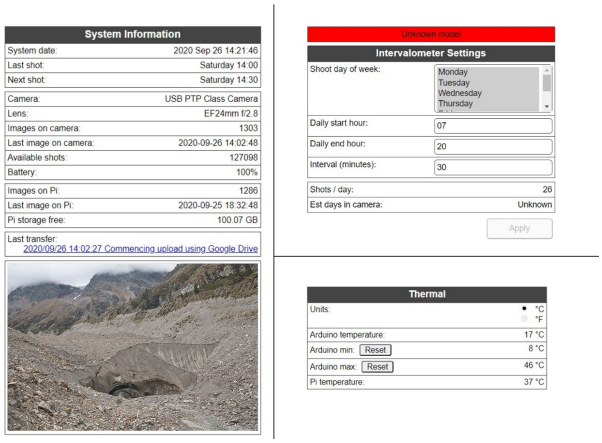

Figure 3. Example of some of the pages of the web-based interface to remotely control the monitoring units.

All the components were chosen because of their low power consumption and their inter-compatibility. The circuit is robust against power losses due to battery discharging and is able to auto-recover when power is regained. A low energy consumption policy is also followed in selecting the scheduling. The camera is switched on only during the data capture activity. The Raspberry is switched on only once per day when the connection with the remote server and image transfer is scheduled.

2.3 Connectivity

Internet connectivity is crucial to transfer images and to control the units remotely. To this end, the Raspberry is equipped with the SIM7600E-H 4G hat by Waveshare. The module supports 4G/3G/2G communication via a SIM card. Raspberry and hat operations are the most expensive in terms of power consumption. For this reason, the board is switched on only once a day for a limited period of time, which is kept adequately low to be sustainable for the system power supply but still sufficient for transferring new images to the server. We adopted IoT (Internet of Things) SIM cards provided by the multi-operator service Emnify (Emnify, 2023), as it offers the ability to connect to the best-quality cellular network available and includes flexible and customizable data plans. Remote access to the devices is allowed by a VPN (Virtual Private Network). The service costs €33 per month for a data plan with 6 GB.

2.4 Case and protection

The majority of the components need to be protected. Therefore, a solid and compact case that allows keeping all the parts (with the exception of the solar panel) in the same location is desirable for the functioning of the system and for convenient transportation, installation and maintenance. The case should also satisfy the thermal insulation requirements according to each component’s working temperature range. The case should also be waterproof and robust against different and harsh weather conditions but, at the same time, provide access for connecting the solar panel and taking pictures. Our choice was an HPRC 2250 lightweight, waterproof resin case with internal insulating foam. The foam was found to be useful in enhancing the temperature seal and stabilising the location of some components, preventing unwanted movements. Holes were drilled in the case: one sealed with a UV filter of 82 mm to allow the camera to take shots, two others to give access to the solar panel wires, and others to fix the system to a tripod. The internal case

dimensions (236x182x155 mm) posed a significant challenge in accommodating all the components inside. In particular, the camera lens dimensions were constrained by space availability.

2.5 General performances

The system was subject to several tests before being used in its final application at the Belvedere glacier site. During these tests, the system proved to be autonomous, robust to sudden shutdowns, cold-resistant, water-resistant and self-sufficient for a prolonged period of time with no direct sunlight on the solar panels. Specifically, in the absence of sunlight, the battery is able to power the system for about nine days before it is completely discharged. Battery voltage and temperatures of components were monitored, simulating the absence of solar radiation and low environmental temperatures. See Figure 4 for the performances of the system during these tests.

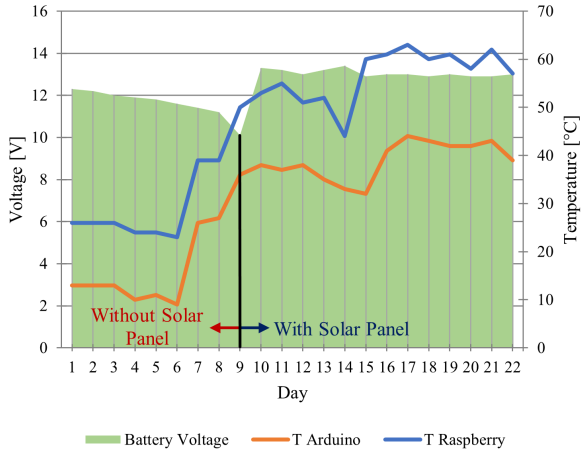

Figure 4. Battery voltage and temperature of boards with and without the solar panel during a period of tests. Starting from a fully charged condition, the system was kept without solar panel at around 2 °C for the first six days. After nine days, the battery was fully discharged and the system was reconnected to the panel and exposed to solar radiation.

It is worth mentioning the performances of the system in terms of costs: our monitoring system can be fully reproduced with an average cost of €1600 per station, including camera (€400), lens (€500) and material for the on-site installation (€150). In comparison, commercial time-lapse cameras (e.g., `https://www.harbortronics.com/Products/TimeLapsePackage`) are expensive ($2,375.00 only for the board) and not adaptable to modifications. The final prototype of the monitoring station is shown in Figure 5.

3. THE BELVEDERE GLACIER CASE STUDY

The system has been tested and it is currently operating (February 2023) at the Belvedere Glacier north-west terminal ice cliff. The Belvedere Glacier is a debris-covered glacier located in Valle Anzasca (Italy), on the east side of the Monte Rosa Massif (located at approximately N 45° 58’, E 7° 55’) (Figure 6). The choice of the Belvedere Glacier was driven by the fact that a long-term monitoring project has been carried out jointly by Politecnico di Milano, Politecnico di Torino and Alta Scuola Politecnica since 2015. The project is aimed at deriving

(a) (b)

Figure 5. (a) Picture of the monitoring unit prototype installed for tests at the Belvedere Glacier site. (b) Picture of the final monumentation of the camera installed on the stream-wise right moraine.

ice flow velocity, volume variations and estimation of the glacier retreat by combining UAV-based photogrammetry, in-situ GNSS measurements (Ioli et al., 2021) and historical aerial photogrammetry (De Gaetani et al., 2021). However, sub-seasonal information on glacier evolution was missing. In this context, a permanent stereoscopic camera system fills this gap.

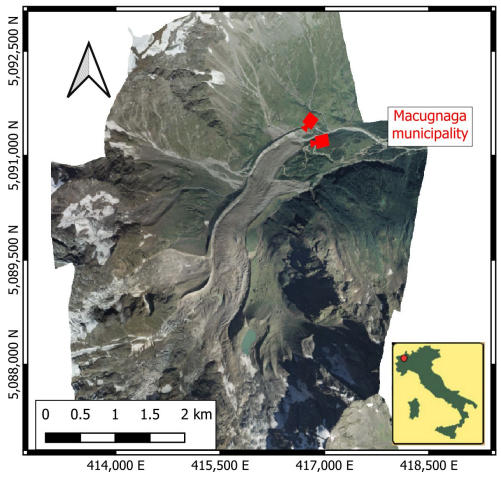

Figure 6. Location of the Belvedere Glacier. The position of the two cameras is marked with red camera symbols.

3.1 Camera and lenses

The choice of the DSLR camera and of the optics can be considered application-dependent. Therefore specifications regarding these components are reported in reference to the Belvedere glacier case study. Each monitoring station was equipped with a DSLR camera Canon EOS 2000D, with 24.1 MP CMOS APS-C sensor. This model was chosen because of the limited costs, the high image resolution and its compactness, as it must fit inside the case. Additionally, another fundamental requirement was camera compatibility with the gPhoto2 software. In the installation inside the system case, the traditional rechargeable battery was replaced by a special battery (”fake

battery”) equipped with a power supply cable, which provides a voltage of 7.5 V from the circuit. The camera is attached to a sliding plate able to vary, with a limited range, and then fix the position of the camera on the longitudinal axis. Screws fix the camera to the plate and the plate to the case.

The two stations were installed respectively at ∼180 m and ∼340 m distance to the glacier terminus (see Figure 7), avoiding the steep moraines of the glacier, often prone to collapses and landslides. Therefore, a wide baseline of ∼260 m occurs between the two sensors. The final positioning of the two cameras was decisive in the choice of optics. In fact, to ensure comparable Ground Sample Distance (GSD) of the images (∼3 cm px^{-1}), lenses with different focal lengths were employed. In particular, a Canon EF 24 mm f/2.8 IS USM and a Canon EF 35 mm f/2 IS USM were used respectively for Camera 1 (stream-wise right) and Camera 2 (stream-wise left).

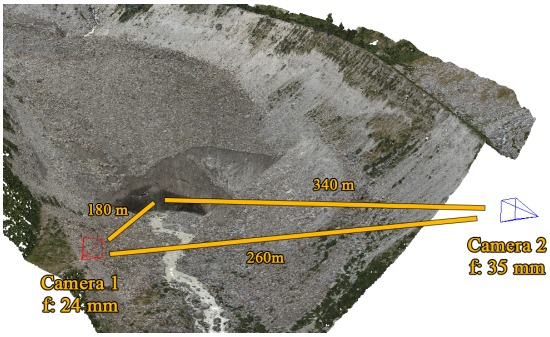

Figure 7. Configuration of cameras installed on the Belvedere glacier. The focal length of each camera is reported next to each camera.

3.2 Monumentation

Monumentation of the two cameras at the Belvedere Glacier site was achieved by choosing two large stable rocks along the moraines. Each camera is supported by an aluminium topographic tripod system anchored with steel dowels and cables to the rocks (Figure 5b). A central steel tie rod keeps the system in a fixed position. The choice of an agile monumentation was aimed at having a system that can be rather easily assembled on site (and also disassembled, if needed), also in a harsh environment, with limited costs and time. To install the cameras, in fact, all the equipment was carried in backpacks along the moraines, sometimes without a marked walking path (e.g., in the case of the stream-wise left camera). As a drawback, the analysis of the acquired photos revealed a non-optimal stabilization of the two cameras. In fact, small rotations, especially around the vertical axis, and vibrations, mostly induced by the wind, were experienced. Though, a perfectly stable monumentation in a mountain environment is hardly achievable. Therefore, it is not possible to assume the camera orientation as stable a priori, but camera orientation must be estimated based on some Ground Control Points (GCPs) located on the ground in stable areas.

3.3 Acquisition performances

The system was installed in August 2021 and is still operating properly (February 2023). Images of the glacier terminus have been collected daily, twice a day, around noon, for more than one year, resulting in ∼ 1000 images collected from each camera. Figure 8 reports an example of a stereo-pair. The two monitoring stations operated almost continuously during this period.

(a) (b)

Figure 8. Example of a stereo-pair of images acquired by the two cameras on 28/07/22 at 14:00. (a) Image taken from Camera 1 (located on the stream-wise right moraine); (b) Image from Camera 2 (stream-wise left moraine).

Figure 9a reports the number of shots per day over a one-year period. The number of shots becomes zero when the monitoring station is inactive due to battery discharging. Figure 9b reports the results of the PVGIS simulation considering a 120 Wh solar panel and daily consumption of 40 Wh, which overestimates the actual daily consumption of the system (Raspberry up-time of hours, several shots per day). The simulation predicts that the battery is fully discharged in 16.87% days of the year. Actual performances revealed that Camera 2 was active on 100% of days and Camera 1 on 90% of days. This is because Camera 2 is situated in a more open area than Camera 1. In fact, Camera 1 is located north of the Belvedere hill which can obstruct the sun’s radiation during the winter months when the sun’s elevation is low.

3.4 Image processing

The daily stereo-pairs are processed by a photogrammetric approach to build 3D models of the glacier terminal ice cliff. The wide baseline between the two cameras, which is typical of complex mountain environments, made it challenging to find corresponding points across different viewpoints (Yao et al., 2021). Indeed, commercial SfM software packages such as Agisoft Metashape (Agisoft Metashape, 2023), as well as an open-source solution such as COLMAP (Schönberger and Frahm, 2016) or MICMAC (Rupnik et al., 2017), which use SIFT (Lowe, 2004) for feature matching, failed to find enough and well-distributed matches. On the other hand, state-of-the-art deep learning-based algorithms for wide-baseline matching, such as SuperGlue (Sarlin et al., 2020), outperformed traditional feature matching. Therefore, a Python routine was developed for finding matches by SuperGlue and performing traditional SfM processing (i.e., relative orientation of the image pair and triangulation of corresponding points). Then, a Bundle Adjustment (BA) was performed with Agisoft Metashape Python API by importing the approximate solution obtained by relative/absolute orientation, as well as a pre-calibrated camera interior orientation. Additionally, the world coordinates of the two cameras, measured by a topographic-grade GNSS receiver, and the coordinates of at least three GCPs (i.e., plastic targets materialized in stable areas along the moraines and measured by GNSS) were included in the BA. Moreover, a dense reconstruction was performed with Agisoft Metashape Python API to build a dense point cloud of the glacier terminus (Figure 10), with $\sim 6 \times 10^6$ pts. Thanks to Agisoft Metashape Python API, Bundle Adjustment and dense reconstruction were fully integrated and automated within the processing workflow.

3.5 Validation with UAV-based Ground Truth

To validate the 3D dense point cloud obtained from the stereo-cameras, Ground Truth (GT) 3D data of the glacier terminus

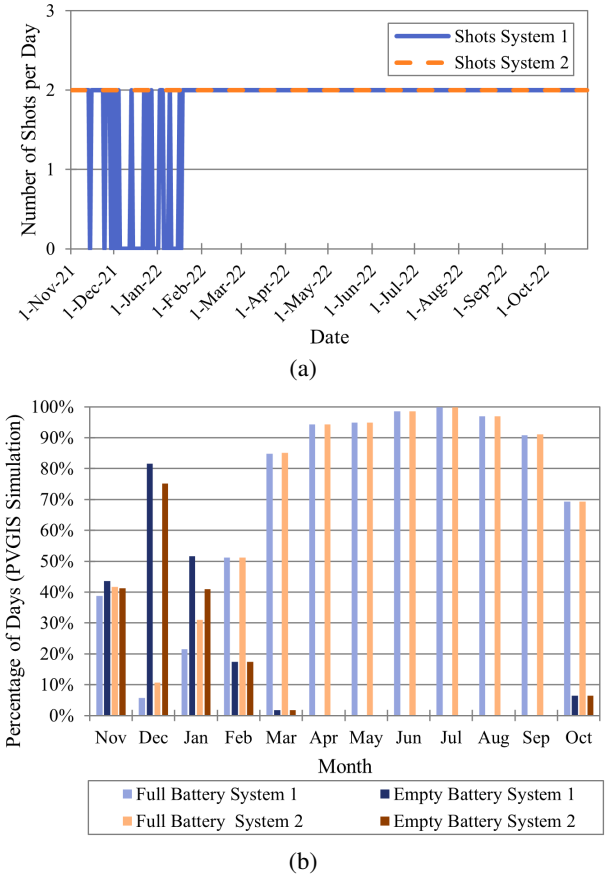

Figure 9. Actual and simulated performances of the system over a year. (a) Number of shots per day of the two systems. (b) Percentage of days in a month when the battery became full or empty according to PVGIS simulations at the location of the two monitoring systems.

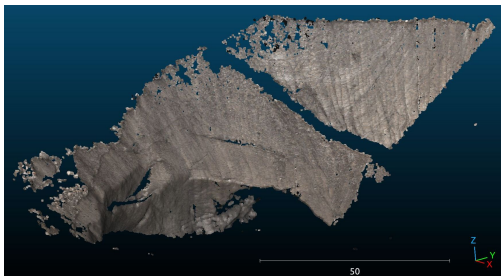

Figure 10. Dense point cloud built from the stereo-pair of 28/07/22. The point cloud was composed of $\sim 6 \times 10^6$ points, with an average point density of $\sim 1000\,\mathrm{pts\,m^{-2}}$.

was acquired on 28/07/2022 by a UAV-based photogrammetric flight, together with 10 GCPs, measured by a GNSS and a total station along the moraines and on the glacier. The images were processed by Agisoft Metashape and the accuracy of the model was evaluated with 5 Check Points (CPs) as an RMSE of $\sim 0.04\,\mathrm{m}$. The dense cloud obtained by the stereo cameras on 28/07/2022 was compared with the concurrent acquired UAV-GT by evaluating the cloud-to-cloud distance along local normals with the M3C2 algorithm (Lague et al., 2013). The resulting differences between the two point clouds, presented in Figure 11, have a mean of $0.01\,\mathrm{m}$ and a standard deviation of $0.08\,\mathrm{m}$, highlighting that there are no systematic errors in the stereo-point cloud and its noise is between 2 and 3 times the average image GSD (i.e., $0.03\,\mathrm{m}$). Considering that the forward speed of the Belvedere Glacier terminus has an average annual velocity of $\sim 0.04\,\mathrm{m\,d^{-1}}$ (Ioli et al., 2021), a time-lag of 3 days may be enough to have a rather good signal-to-noise ratio when comparing two consecutive stereo-point clouds.

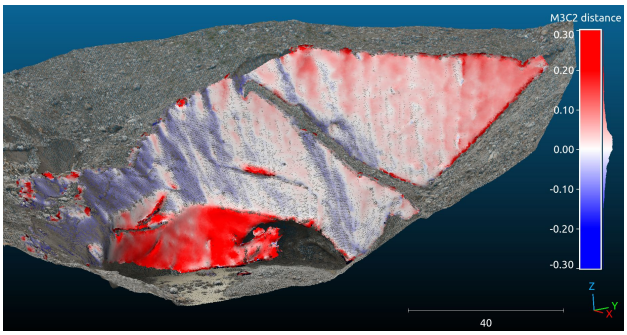

Figure 11. Cloud-to-cloud distances, computed with M3C2 algorithm, between the UAV-based ground truth point cloud (displayed with RGB colors) and the stereo-point cloud (displayed with a color scale). The colors represent the average distance (i.e., error) between each point of the stereo-point cloud (seed point) and the points of the UAV cloud that falls within a cylinder oriented as the local normal computed around the seed point. Most of the points have an error smaller than $\pm 10\,\mathrm{cm}$, with the highest values concentrated within the cave.

3.6 Volume variations

From a pair of stereo-points clouds built on different days, the glacier terminus retreat was obtained by computing cloud-to-cloud distances with M3C2. As an example, Figure 12 presents the distances between the stereo-point cloud obtained on 28/07/22 and that obtained one month later on 30/08/22, resulting in an average retreat of $2.7\,\mathrm{m}$. Integrating the displacement over the area in which both point clouds contain points and normalizing the result by the whole area covered by the glacier ice cliff, it was possible to estimate the ice volume variation. Between 28/07/22 and 30/08/22, $\sim 14 \times 10^3\,\mathrm{m^3}$ of ice volume was lost. The same procedure can be applied to the whole time series of data by choosing a proper time step between point cloud pairs, i.e., small enough to appreciate sub-weekly variations but maintaining a good signal-to-noise ratio when computing the displacements.

4. DISCUSSIONS AND FUTURE PERSPECTIVES

The low-cost stereoscopic system proposed in this study demonstrates accurate and robust performance, as it has been collecting daily data from the Belvedere Glacier for more than a year (August 2021-February 2023). The camera system can stand the extreme mountain environment, being weather- and cold-resistant. Its low power consumption sustained by solar panels allowed an autonomous functioning for the whole acquiring period. And these performances were achieved with easy assembly and low-cost components. Thanks to its characteristics, the system performed better than expected. The percentage of days in which the collection of data was prevented by battery discharging was at least 5% lower than the PVGIS simulation prediction. However, the system can be improved in various ways. One is the optimization of the camera's stabilization and the positioning of the tripod. Moreover, the system

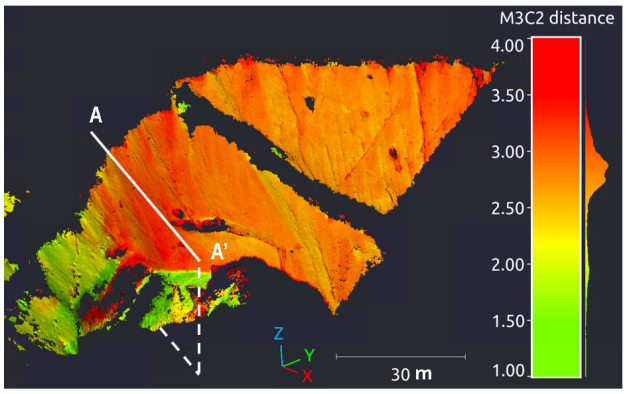

(a)

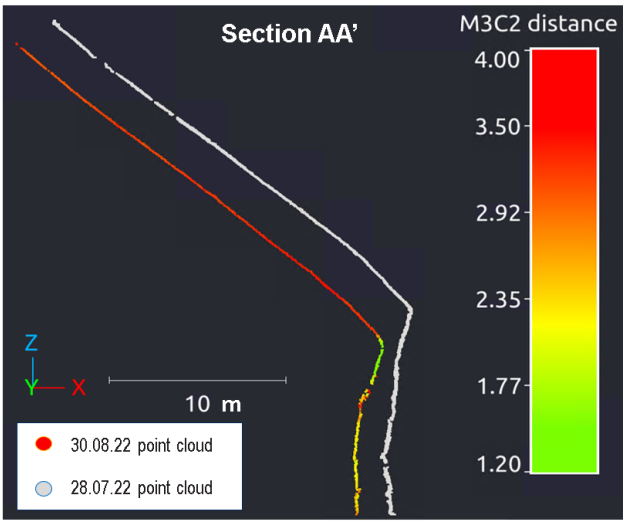

(b)

Figure 12. (a) Glacier terminus retreat between 28/07/22 and 30/08/22, computed as M3C2 cloud-to-cloud distances between stereo-point clouds. The colors represent the distances between each point of the 30/08/22 point cloud (seed point) and the points of 28/07/22 that fall within a cylinder oriented as the local normal computed around the seed point. Distances are expressed in meters. (b) Computed distances extracted along the transversal cross-section AA'. The 28/07/22 point cloud is represented with a gray color as a reference.

could be made even more autonomous, making it independent of mobile networks, which coverage can be unreliable and often missing in alpine environments.

A multi-camera system allows for computing glacier retreat and volume variations in a 3D world, which is not achievable with monoscopic camera systems. Information about the ice volume lost can be combined with ablation (estimated as a reduction of the height of the glacier surface from 3D point clouds) and ice flow velocity information, e.g., derived from single camera time-series by DIC (Messerli and Grinsted, 2015, Schwalbe and Maas, 2017, How et al., 2020), to gather a complete understanding of the glacier dynamics. Furthermore, multi-camera systems do not need any a priori information for reconstructing 3D scenes, overcoming the limit of monoscopic systems that require DEMs to translate 2D pixel displacements computed by DIC to 3D displacement vectors. If a complete DEM of the glacier surface can be reconstructed at each epoch by stereo-cameras, it can be used to derive 3D metric displacements, as proposed by Marsy et al. (Marsy et al., 2020). Otherwise, if the camera viewshed is limited (as for the Belvedere Glacier case study), information about the glacier ablation at the terminal ice cliff can be employed to model the evolution of a glacier DEM (e.g., acquired by UAV) over time.

Although the results of the stereoscopic system are promising, the routine for processing stereo-pairs and extracting relevant information (e.g., volume losses, flow velocities) from point cloud series is still under active development. In particular, alternative open-source solutions for performing BA and dense reconstructions are under study to replace the commercial software Agisoft Metashape. Moreover, change detection algorithms such as M3C2 (Lague et al., 2013), or its improved variations such as CDPB-M3C2 (Zahs et al., 2022), for increasing the signal-to-noise ratio when changes have magnitude similar to the uncertainty, are being tested. The focus of this paper, however, is on the hardware implementation of a low-cost multi-camera monitoring system rather than on image processing methods and results obtained on the Belvedere Glacier. Therefore, a thorough discussion of the processing methods and analysis of the results will be addressed in a future paper, and all the Python routines will be published in an open-source repository. Additionally, in the case study of the Belvedere Glacier, only two cameras were employed. However, the system can be easily extended to include multiple cameras for increasing viewing coverage, which may allow for deriving a full DEM of the area of interest, without limiting the reconstruction to the terminal ice cliff only.

5. CONCLUSIONS

This paper presents a low-cost implementation of an image-based stereoscopic system for continuous glacier monitoring. The system is composed of two autonomous monitoring units that are designed and built with low-cost and off-the-shelves components and can be easily replicated (and possibly also improved) by non-experts. Each monitoring unit includes a DSLR camera, an Arduino Pro Mini microcontroller for camera triggering and waking up the system and a Raspberry Pi Zero W board for storing the images taken by the camera, providing remote access to the system by internet connection and automatically sending the images to a remote server. The system has its autonomous power supply, ensured by a lead-acid battery and a solar panel, and it is enclosed in a waterproof case. The total cost of a single monitoring unit, including a middle-edge DSRL camera with a fixed-focal-length lens, was between €1500 and €2000. This, together with the easy implementation, makes the system affordable and reproducible for several remote glacier sites.

From daily stereo-pairs, 3D dense point clouds of the glacier terminus can be built with decimetric accuracy and used for estimating glacier retreat over time, ice volume loss and applying change detection algorithms on point clouds, with sub-weekly frequency. Especially if combined with forward glacier surface velocity, information regarding glacier retreat and ice volume losses over time is extremely valuable information for glaciologists who are aimed at understanding sub-seasonal glacier dynamics and computing mass balances.

6. ACKNOWLEDGMENTS

The stereoscopic system was designed, realized and deployed at Belvedere Glacier within the Alta Scuola Politecnica (ASP), a joint venture between Politecnico di Milano

and Politecnico di Torino, through the multidisciplinary project titled "Kuoleva Jaatikko" (https://www.asp-poli.it/kuoleva-jäätikkö/). Many thanks are owed to Iosif Horea Bendea for the realization of the monumentation system and his work on the cases of the two monitoring units. We thank Paolo Maschio and Fabio Giulio Tonolo for their fruitful suggestion in the design phase and their help in the installation. We finally thank the Belvedere ropeway team and all the people of Macugnaga municipality who made with their help possible the transportation and installation of the monitoring systems.

REFERENCES

Agisoft Metashape, 2023. [Online; visited on 22/2/2023].

Barry, R. G., 2006. The status of research on glaciers and global glacier recession: a review. *PPG: Earth and Environment*, 30(3), 285-306.

Chudley, T. R., Christoffersen, P., Doyle, S. H., Abellan, A., Snooke, N., 2019. High-accuracy UAV photogrammetry of ice sheet dynamics with no ground control. *Cryosphere*, 13(3), 955–968.

De Gaetani, C. I., Ioli, F., Pinto, L., 2021. Aerial and UAV Images for Photogrammetric Analysis of Belvedere Glacier Evolution in the Period 1977–2019. *Remote Sens.*, 13(18), 3787.

Dematteis, N., Giordan, D., Crippa, B., Monserrat, O., 2022. Fast local adaptive multiscale image matching algorithm for remote sensing image correlation. *Computers & Geosciences*, 159, 104988.

Eltner, A., Kaiser, A., Abellan, A., Schindewolf, M., 2017. Time lapse structure-from-motion photogrammetry for continuous geomorphic monitoring. *Earth Surf. Proc. Land.*, 42(14), 2240-2253.

Emnify, 2023. [Online; visited on 22/2/2023].

EU Science Hub, 2022. Photovoltaic Geographical Information System (PVGIS). https://joint-research-centre.ec.europa.eu/pvgis-online-tool_en.

Giordan, D., Allasia, P., Dematteis, N., Dell’Anese, F., Vagliasindi, M., Motta, E., 2016. A low-cost optical remote sensing application for glacier deformation monitoring in an alpine environment. *Sensors*, 16(10), 1750.

How, P., Hulton, N. R. J., Buie, L., Benn, D. I., 2020. PyTrx: A Python-Based Monoscopic Terrestrial Photogrammetry Toolset for Glaciology. *Frontiers Earth Scie.*, 8.

Ide, R., Oguma, H., 2013. A cost-effective monitoring method using digital time-lapse cameras for detecting temporal and spatial variations of snowmelt and vegetation phenology in alpine ecosystems. *Ecological Informatics*, 16, 25-34.

Ioli, F., Bianchi, A., Cina, A., De Michele, C., Maschio, P., Passoni, D., Pinto, L., 2021. Mid-Term Monitoring of Glacier’s Variations with UAVs: The Example of the Belvedere Glacier. *Remote Sens.*, 14(1), 28.

James, M. R., How, P., Wynn, P. M., 2016. Pointcatcher software: analysis of glacial time-lapse photography and integration with multitemporal digital elevation models. *J. Glaciol.*, 62(231), 159–169.

Kneib, M., Miles, E. S., Buri, P., Fugger, S., McCarthy, M., Shaw, T. E., Chuanxi, Z., Truffer, M., Westoby, M. J., Yang, W., Pellicciotti, F., 2022. Sub-seasonal variability of supraglacial ice cliff melt rates and associated processes from time-lapse photogrammetry. *The Cryosphere*, 16(11), 4701–4725.

Lague, D., Brodu, N., Leroux, J., 2013. Accurate 3D comparison of complex topography with terrestrial laser scanner: Application to the Rangitikei canyon (NZ). *ISPRS J. Photogramm. Remote Sens.*, 82, 10–26.

Lowe, D. G., 2004. Distinctive image features from scale-invariant keypoints. *Int. J. Comput. Vision*, 60(2), 91–110.

Marsy, G., Vernier, F., Bodin, X., Cusicanqui, D., Castaings, W., Trouvé, E., 2020. Monitoring mountain cryosphere dynamics by time lapse stereo photogrammetry. *ISPRS Ann. Photogramm. Remote Sens. Spat. Inf. Sci.*, V-2.

Messerli, A., Grinsted, A., 2015. Image georectification and feature tracking toolbox: ImGRAFT. *Geosci. Intrum. Meth.*, 4(1), 23–34.

Piermattei, L., Carturan, L., De Blasi, F., Tarolli, P., Dalla Fontana, G., Vettore, A., Pfeifer, N., 2016. Suitability of ground-based SfM-MVS for monitoring glacial and periglacial processes. *Earth Surf. Dynam*, 4, 425–443.

Roncella, R., Forlani, G., Fornari, M., Diotri, F., 2014. Landslide monitoring by fixed-base terrestrial stereophotogrammetry. *ISPRS Ann. Photogramm. Remote Sens. Spat. Inf. Sci.*, 2(5), 297–304.

Rupnik, E., Daakir, M., Pierrot Deseilligny, M., 2017. MicMac–a free, open-source solution for photogrammetry. *Open Geospat. Data, Softw. Stand.*, 2(1), 1–9.

Sarlin, P.-E., DeTone, D., Malisiewicz, T., Rabinovich, A., 2020. SuperGlue: Learning feature matching with graph neural networks. *Proc. CVPR IEEE*.

Schönberger, J. L., Frahm, J.-M., 2016. Structure-from-motion revisited. *Proc. CVPR IEEE*.

Schwalbe, E., Maas, H.-G., 2017. The determination of high-resolution spatio-temporal glacier motion fields from time-lapse sequences. *Earth Surf. Dynam.*, 5(4), 861–879.

Sheridan, G., 2021. Intervalometerator Version 4.4.3. https://github.com/greiginsydney/Intervalometerator.

Vallot, D., Adinugroho, S., Strand, R., How, P., Pettersson, R., Benn, D. I., Hulton, N. R. J., 2019. Automatic detection of calving events from time-lapse imagery at Tunabreen, Svalbard. *Geosci. Intrum. Meth.*, 8(1), 113–127.

Yao, G., Yilmaz, A., Meng, F., Zhang, L., 2021. Review of Wide-Baseline Stereo Image Matching Based on Deep Learning. *Remote Sens.*, 13(16), 3247.

Young, D. S., Hart, J. K., Martinez, K., 2015. Image analysis techniques to estimate river discharge using time-lapse cameras in remote locations. *Computers & Geosciences*, 76, 1–10.

Zahs, V., Winiwarter, L., Anders, K., Williams, J. G., Rutzinger, M., Höfle, B., 2022. Correspondence-driven plane-based M3C2 for lower uncertainty in 3D topographic change quantification. *ISPRS J. Photogramm. Remote Sens.*, 183, 541–559.

Zemp, M., Haeberli, W., Hoelzle, M., Paul, F., 2006. Alpine glaciers to disappear within decades? *Geophys. Res. Lett.*, 33(13).